Journal of Alloys and Compounds 509 (2011) 7016–7021

Contents lists available at ScienceDirect

Journal of Alloys and Compounds

journal homepage: www.elsevier.com/locate/jallcom

Cobalt–nickel–phosphorus supported on Pd-activated TiO_2 (Co–Ni–P/Pd-TiO_2) as cost-effective and reusable catalyst for hydrogen generation from hydrolysis of alkaline sodium borohydride solution

Murat Rakap[a,b,1], Egwu Eric Kalu[a,*], Saim Özkar[b]

[a] Department of Chemical and Biomedical Engineering, FAMU-FSU College of Engineering, Tallahassee, FL 32312, USA
[b] Department of Chemistry, Middle East Technical University, 06800 Ankara, Turkey

ARTICLE INFO

Article history:
Received 7 March 2011
Accepted 1 April 2011
Available online 9 April 2011

Keywords:
Cobalt
Nickel
Sodium borohydride
Hydrolysis
Hydrogen generation

ABSTRACT

Catalytically active, low-cost, and reusable transition metal catalysts are desired to develop on-demand hydrogen generation system for practical onboard applications. Electrolessly deposited Pd-activated TiO_2-supported Co–Ni–P ternary alloy catalyst (Co–Ni–P/Pd-TiO_2) is employed as catalyst in the hydrolysis of alkaline sodium borohydride solution. The catalyst is found to be isolable, redispersible, and reusable in the hydrolysis of alkaline $NaBH_4$. The reported work also includes the full experimental details for the collection of a wealth of kinetic data to determine the activation energy (E_a = 57.0 kJ/mol) and effects of the amount of catalyst, amount of substrate, and temperature on the rate for the catalytic hydrolysis of $NaBH_4$. Maximum H_2 generation rate of ~460 mL H_2 min^{-1} (g catalyst)$^{-1}$ and ~3780 mL H_2 min^{-1} (g catalyst)$^{-1}$ was measured by the hydrolysis of $NaBH_4$ at 25 °C and 55 °C, respectively.

1. Introduction

The concerns over the depletion of fossil fuels supplies and the environmental pollution and global warming attributable to the greenhouse effect caused by a steep increase in carbon dioxide and other gases have made hydrogen one of the most promising future energy resources [1–3]. However, the development of effective and safe hydrogen storage materials is the most important challenge toward hydrogen powered society as a long-term solution for a secure energy future [4,5]. The chemical hydrogen storage, in which hydrogen is stored in chemical compounds such as $NaBH_4$, H_3NBH_3, LiH, NaH, CaH_2, MgH_2, $LiAlH_4$, etc. [6,7], and released via an irreversible chemical reaction, is a promising strategy [8]. Among the chemical hydrides, sodium borohydride ($NaBH_4$) has received the most extensive attention owing to its combined advantages of: (i) the high hydrogen storage capacity (10.8 wt.%); (ii) the high stability and nonflammability of its alkaline solutions; (iii) the optimal control on hydrogen generation rate by supported catalysts; (iv) the acceptable hydrogen generation rate even at low temperature; (v) the availability and easy handling [9], (vi) an efficient hydrogen source which releases hydrogen gas in the amount double of its hydrogen content upon hydrolysis in water (Eq. (1)) [10]:

$$NaBH_4(aq) + 2H_2O(l) \xrightarrow{\text{catalyst}} NaBO_2(aq) + 4H_2(g) \tag{1}$$

Although the self hydrolysis of sodium borohydride at room temperature is quite slow, it can be completely suppressed by working in highly basic solution [11]. Thus, the hydrolysis of sodium borohydride occurs only in the presence of a suitable catalyst [12]. Various catalysts including ruthenium [12], Pt/$LiCoO_2$ [13], carbon supported platinum [14], PtRu/$LiCoO_2$ [15], Ru/IRA-400 [16], Ru(0) nanoclusters [17], nickel [18], electrodeposited Co and Co–P [19], Co/γ-Al_2O_3 [20], hydrogenphosphate-stabilized nickel(0) nanoclusters [21], Co–B [22], Pt/C [23], nickel–cobalt–boride [24], Co–Mn–B nanocomposite [25], cobalt–boron/nickel foam [26], Ru/$LiCoO_2$ [27], cobalt–tungsten–boron/nickel foam [28], Co/C [29], electrolessly deposited Co–P [30], Ru/γ-Al_2O_3 [3], PVP-stabilized nickel(0) nanoclusters [31], Co–B/MWCN [32], Ru-promoted sulphated zirconia [33], Ni–Ru nanocomposite [34], fluorinated cobalt [35], PtPd–carbon nanotubes [36], aluminum chloride [37], acetic acid [38], intrazeolite cobalt(0) nanoclusters [39], polymer-stabilized cobalt(0) nanoclusters [40], Co–Cr–B [41], porous Fe–Co–B/Ni foam [8], Ru/Graphite [42], clay-supported Co–B [43], Co–Ni–B [44], attapulgite CoB [45], Co–Cu–B [46], Pd/C [47], Ni_xB [48], Co-powder [49], Ru/IR-120 [50], BMR07 (Ni based) [51], Ru/C [52], Ru–Pd–Pt [53], mono- and di-carboxylic acids [54], zeolite framework stabilized nickel(0) nanoparticles [55], and $Mm(Ni_{3.6}Co_{0.7}Mn_{0.4}Al_{0.3})_{1.15}$ hydride electrodes [56] have been

---

* Corresponding author at: Florida A&M University, Chemical and Biomedical Engineering, 2525 Pottsdamer Street, Tallahassee, FL 32310, USA. Tel.: +1 850 410 6327; fax: +1 850 410 6150.
E-mail address: ekalu@eng.fsu.edu (E.E. Kalu).

[1] On leave of absence from Department of Chemistry, Yüzüncü Yıl University, 65080 Van, Turkey.

0925-8388/$ – see front matter © 2011 Elsevier B.V. All rights reserved.
doi:10.1016/j.jallcom.2011.04.023

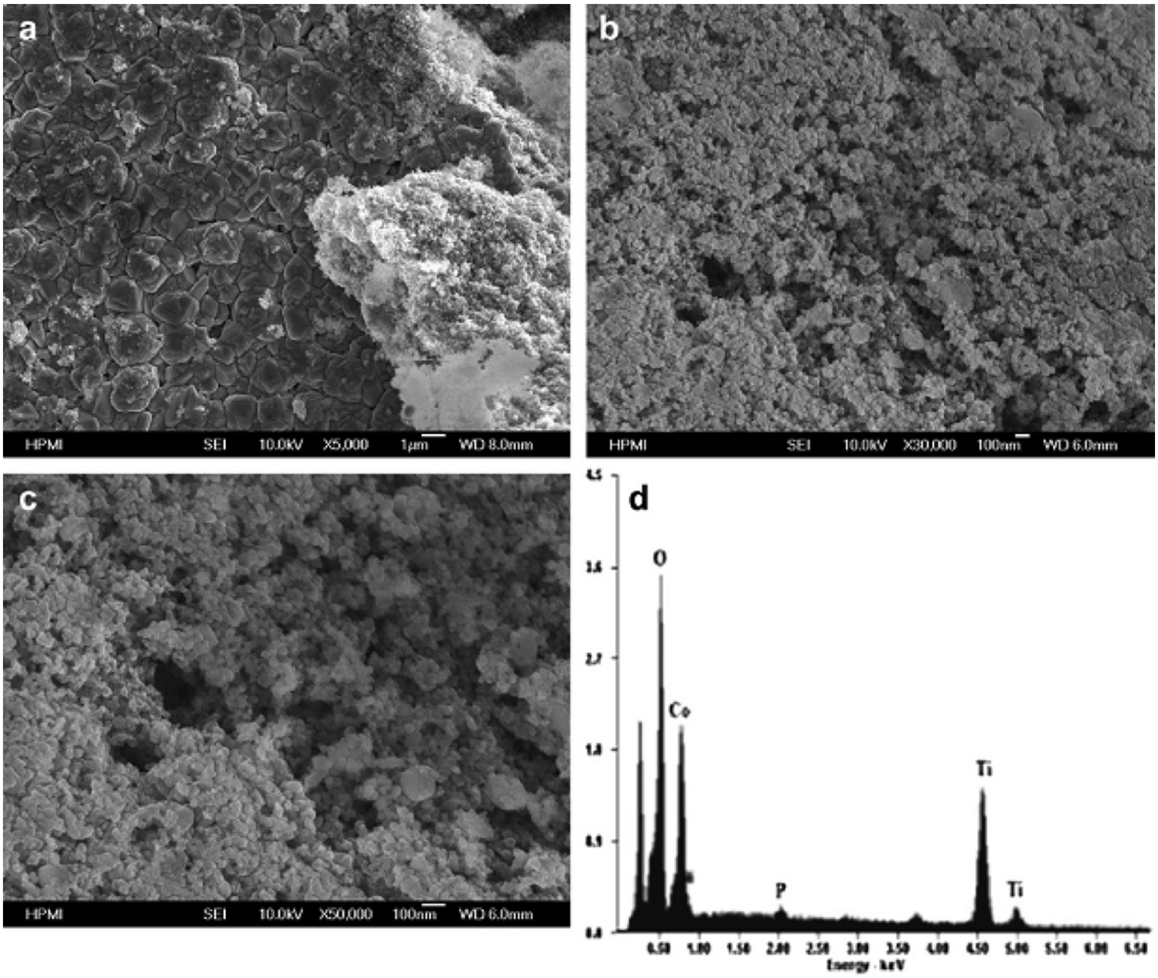

Fig. 1. The SEM micrographs of the surface morphologies of the electroless Co–Ni–P ternary alloy deposit on Pd-TiO_2 at magnifications of: (a) 5000, (b) 30,000, and (c) 50,000, and (d) the EDX micrograph.

tested as the catalysts to accelerate the hydrolysis of $NaBH_4$. In general, precious metal catalysts show excellent activity in hydrogen generation from the hydride compounds while their use in practical applications is restricted by their high material cost. On the other hand, the cheaper transition metal catalysts generally exhibit only moderate catalytic activity. Therefore, the development of low-cost and efficient catalyst is desired for practical use. Recent advances in catalyst preparation technologies have led to significant improvements in the catalytic activity of transition metal catalysts, even to a level comparable to that of the noble metal catalysts [26]. In particular, the supported non-noble transition metals can be employed as active catalysts in practical applications owing to their easy separation from the solution and reusability of the catalysts [2].

Indeed, our recent study [57] has shown that Co–Ni–P catalyst prepared by electroless deposition method on the surface of Pd-activated TiO_2 (Co–Ni–P/Pd-TiO_2) can be used as active catalyst in the hydrolysis of ammonia–borane. This has stimulated us to use Co–Ni–P as catalyst for hydrogen generation from the hydrolysis of $NaBH_4$. Herein, we report the use of Co–Ni–P as catalyst in the hydrolysis of $NaBH_4$. Co–Ni–P catalyst was found to be highly active catalyst in the hydrolysis of $NaBH_4$, too. The present work presents the results and discussion on the activity of the catalyst in hydrogen generation from the hydrolysis of alkaline $NaBH_4$, as well as the results of kinetic study on the catalytic reaction depending on the catalyst concentration, substrate concentration, and temperature.

2. Experimental

2.1. Chemicals

Cobalt sulphate heptahydrate, nickel sulphate hexahydrate, sodium hypophosphite monohydrate, EDTA, gluconic acid, boric acid, ammonium hydroxide, sodium potassium tartrate, sodium borohydride (99%), sodium hydroxide, palladium acetate, butvar (B98), and titanium dioxide (Degussa P-25) were purchased from Aldrich. All chemicals were used as received. Deionized water was distilled by water purification system.

2.2. Preparation of the Co–Ni–P/Pd-TiO_2 catalyst

The Co–Ni–P catalyst was prepared and supported on Pd-TiO_2 by using electroless deposition method [57]. Briefly, titanium dioxide-catalyst ink (1:12) mixture was stirred to prepare Pd-activated TiO_2 (Pd-TiO_2) for 2 h at room temperature, and kept at 270 °C for 48 h and then 350 °C for 6 h. To initiate the electroless deposition process, 0.2 g of activated titanium dioxide (Pd-TiO_2) was added into the 25 mL of electroless plating bath solution. The electroless Co–Ni–P particle deposition was conducted for 30 min. The reaction was then terminated by rapid cooling of plating bath with the addition of cold water. These Co–Ni–P/Pd-TiO_2 particles were easily collected by centrifugation, and then washed with deionized water and methanol before drying in the oven at 50 °C.

2.3. Method to test the catalytic activity of Co–Ni–P/Pd-TiO_2 catalyst in the hydrolysis of sodium borohydride

The catalytic activity of electrolessly deposited Co–Ni–P/Pd-TiO_2 catalyst in the hydrolysis of $NaBH_4$ was determined by measuring the rate of hydrogen generation. In all the experiments, the reaction flask (30 mL) was placed in a thermostat that was equipped with a water circulating system, wherein the temperature was kept constant at 25 ± 0.5 °C [57]. Then, a graduated burette (50 mL) filled with water was connected to reaction flask to measure the volume of the hydro-

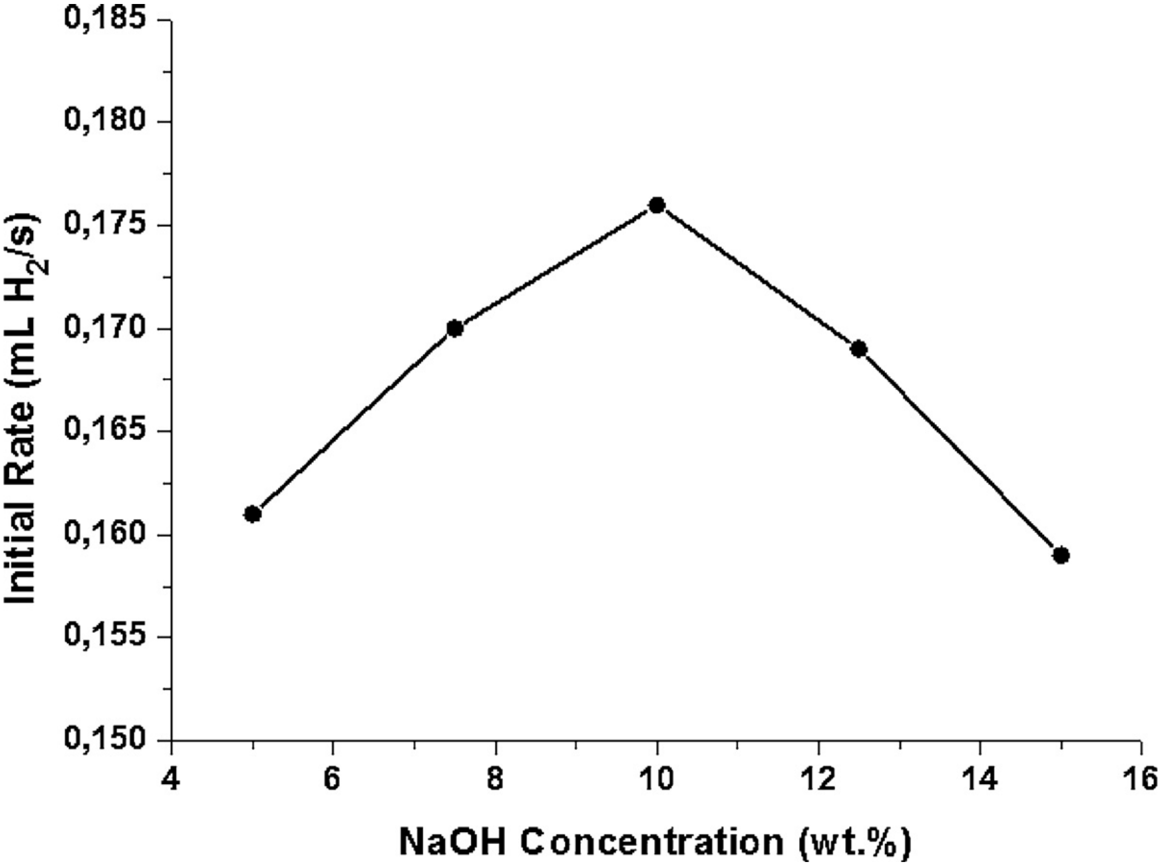

Fig. 2. Plot of the initial hydrogen generation rate versus concentration of NaOH (in wt.%) for the hydrolysis of sodium borohydride (20 mL, 300 mM $NaBH_4$) catalyzed by Co–Ni–P/Pd-TiO_2 catalysts (25 mg) at 25.0 ± 0.5 °C.

gen gas to be evolved from the reaction. Next, 227 mg (6 mmol, 300 mM) $NaBH_4$ was dissolved in 20 mL water (corresponding to 24 mmol = 538 mL H_2). The solution was transferred with a glass-pipette into the reaction flask thermostated at 25.0 ± 0.5 °C. Then, certain amount of Co–Ni–P/Pd-TiO_2 (25, 50, 75, and 100 mg, respectively) catalyst was added into the reaction flask. The reaction was started by closing the flask and the volume of hydrogen gas evolved was measured by recording the displacement of water level from the graduated burette as the reaction progressed.

2.4. Effect of sodium hydroxide concentration on hydrogen generation rate

In order to study the effect of NaOH concentration on the catalytic activity of Co–Ni–P/Pd-TiO_2 catalyst in the hydrolysis of sodium borohydride (300 mM), catalytic activity tests were carried out at 25.0 ± 0.5 °C by changing the concentration of NaOH (5.0, 7.5, 10.0, 12.5, and 15.0 wt.%). In all the experiments, the total volume of solution was kept constant at 20 mL. All the experiments were performed in the same way as described in Section 2.3. The highest activity of Co–Ni–P/Pd-TiO_2 catalyst in the hydrolysis of sodium borohydride was obtained when 10 wt.% NaOH was used. Thus, the concentration of NaOH of 10 wt.% was selected for the further experiments.

2.5. Kinetic study of the hydrolysis of sodium borohydride catalyzed by Co–Ni–P/Pd-TiO_2 catalyst

In order to establish the rate law for catalytic hydrolysis of basic $NaBH_4$ solution containing 10 wt.% NaOH using Co–Ni–P/Pd-TiO_2 as catalyst, two different sets of experiments were performed in the same ways described in Section 2.3. In the first set of experiments, the hydrolysis reaction was carried out starting with different initial amounts of catalyst (25, 50, 75, and 100 mg) and keeping the initial sodium borohydride concentration constant at 300 mM. The second set of experiments was carried out by keeping the initial amount of catalyst constant (25 mg) and varying the $NaBH_4$ concentration of 300, 450, 600 and 750 mM. Finally, the catalytic hydrolysis of $NaBH_4$ was carried out by keeping the amounts of Co–Ni–P/Pd-TiO_2 catalyst (25 mg) and $NaBH_4$ substrate (300 mM) constant at temperatures of 25, 35, 45, and 55 °C in order to obtain the activation energy (E_a) for this hydrolysis reaction.

2.6. Reusability of Co–Ni–P/Pd-TiO_2 catalyst in the hydrolysis of sodium borohydride

After the hydrolysis reaction of sodium borohydride (227 mg, 300 mM) in the presence of NaOH (10 wt.%) was completed, the catalyst (25 mg) was filtered, washed with deionized water and dried in the oven at 100 °C. Then, another equivalent of aqueous $NaBH_4$ solution was added to the reaction flask which contained the catalyst. The released hydrogen gas was then monitored by the gas burette. Such reusability experiments were repeated for 5 times under ambient atmosphere at room temperature.

2.7. Catalyst characterization

Powder X-ray diffraction (XRD) patterns were recorded with a Rigaku X-ray Diffractometer using Cu Kα radiation (30 kV, 15 mA) at room temperature. Scanning was performed between 2θ degrees of 20–80°. The measurements were made with 0.01 and 0.05 degree steps and 1 degree/minute rate. The divergence slit was variable and scattering and receiving slit were 4.2 degree and 0.3 mm, respectively. Scanning Electron Microscopy (SEM) analysis was carried out with a Zeiss 1540 ESB scanning electron microscope operating at an accelerating voltage of 10 kV, equipped with an energy dispersive X-ray (EDX) analysis unit.

3. Results and discussion

3.1. Characterization of the catalyst

The detailed information on the preparation and characterization of the Co–Ni–P/Pd-TiO_2 catalyst prepared using the electroless deposition method can be found elsewhere [57]. Representations of the SEM morphologies of the catalyst at varied magnifications along with the EDX micrograph are shown in Fig. 1. From this figure, it can be concluded that the catalyst shows agglomerated particle-like morphology with the primary particles ranging in size from 20 to 30 nm. Some of the agglomerated particles fall outside the 30 nm range reaching up to 80 nm. The electroless Co–Ni

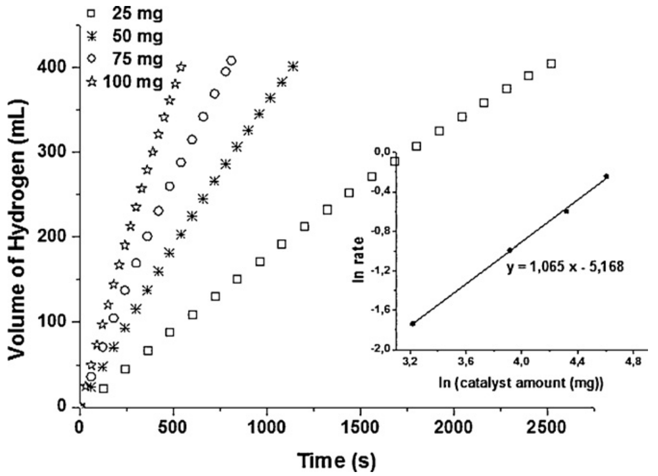

Fig. 3. . Plot of the volume of H_2 (mL) versus time (s) for the hydrolysis of $NaBH_4$ (300 mM) catalyzed by Co–Ni–P/Pd-TiO_2 catalysts with different amounts of catalyst at 25 ± 0.5 °C. The inset shows the plot of the hydrogen generation rate versus the amount of catalyst (both in logarithmic scale) for the same reaction.

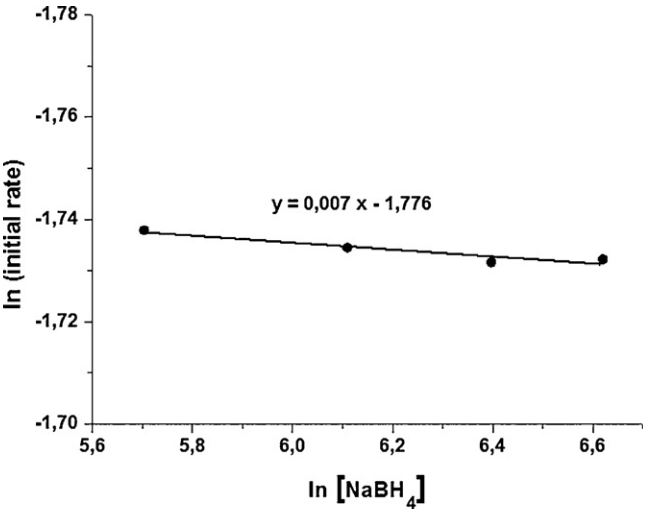

Fig. 4. Plot of the initial hydrogen generation rate versus $NaBH_4$ concentration (both in logarithmic scale) for the hydrolysis of $NaBH_4$ catalyzed by Co–Ni–P/Pd-TiO_2 catalyst (25 mg) in the presence of different $NaBH_4$ concentrations of at 25 ± 0.5 °C.

appears to have coated the Pd-TiO_2 substrate uniformly. At the lower magnifications, the particles are seen to be mostly non-spherical. The EDX micrograph shows the average composition (Co:Ni:P = 94:5.3:0.7 wt.%) taken at multiple points on the sample.

3.2. *Effect of sodium hydroxide concentration on the hydrogen generation rate*

Fig. 2 shows the plot of initial hydrogen generation rate versus concentration of NaOH in wt.% for the hydrolysis reaction of $NaBH_4$ catalyzed by Co–Ni–P/Pd-TiO_2 catalyst. The initial rate of hydrogen generation first increases with the increasing sodium hydroxide concentration, demonstrating an enhancement of reaction by NaOH. It reaches a maximum value at the concentration of 10 wt.% NaOH and subsequently decreases with further increase in NaOH concentration. This is probably due to the fact that OH^- ion is involved in the hydrolysis of $NaBH_4$ and an appropriate increase in the NaOH concentration can accelerate the hydrolysis reaction and thus hydrogen generation rate. However, excessive NaOH concentration would lead to a decrease in solubility of the hydrolysis by-product, $NaBO_2$. As a result, $NaBO_2$ precipitates from the solution and decreases the hydrogen generation rate, blocking the active sites on the surface of the catalyst [46]. Since similar results have been reported [39,46] for some cobalt-based catalysts used for hydrogen generation from the hydrolysis of sodium borohydride, it can be concluded that the hydrogen generation rate is not only dependent on the sodium hydroxide concentration of the solution but also on the nature of the catalyst. As implied by the plot of the catalytic activity versus sodium hydroxide concentration (in wt.%), all the subsequent experiments were performed in solutions containing 10 wt.% NaOH.

3.3. *Kinetic study of the hydrolysis of sodium borohydride catalyzed by Co–Ni–P/Pd-TiO_2 catalyst*

The kinetics of the hydrolysis of $NaBH_4$ catalyzed by the Co–Ni–P/Pd-TiO_2 catalyst was studied with regard to the amount of catalyst used, amount of $NaBH_4$ used, and temperature. Fig. 3 shows the plot of the volume of hydrogen gas generated from the hydrolysis of $NaBH_4$ solution versus time in the presence of different amounts of Co–Ni–P/Pd-TiO_2 catalyst at 25 ± 0.5 °C. The inset in Fig. 3 shows the plot of the initial hydrogen generation rate versus the amount of catalyst (both in logarithmic scale) for the same reaction. The slope of the straight line is 1.07, indicating that the hydrolysis reaction is first order with respect to the amount of Co–Ni–P/Pd-TiO_2 catalyst.

The effect of $NaBH_4$ concentration on the hydrogen generation rate was also studied by carrying out a series of experiments starting with various initial concentration of $NaBH_4$ in the range 300–750 mM while keeping the amount of Co–Ni–P/Pd-TiO_2 catalyst constant (25 mg). Fig. 4 shows the plot of the initial hydrogen generation rate versus the concentration of $NaBH_4$ (both in logarithmic scale) for the hydrolysis of $NaBH_4$ solution in the presence of different initial concentration of $NaBH_4$ at 25 ± 0.5 °C. From this figure, it is concluded that the hydrolysis reaction is practically independent of the $NaBH_4$ concentration, at least in the range 300–750 mM. Consequently, the rate law for the catalytic hydrolysis of $NaBH_4$ can be given as in Eq. (2)

$$\frac{-4d\,[\mathrm{NaBH_4}]}{dt} = \frac{d\,[\mathrm{H_2}]}{dt} = k[\mathrm{Catalyst}] \tag{2}$$

Then, the hydrolysis of $NaBH_4$ catalyzed by Co–Ni–P/Pd-TiO_2 catalyst was carried out at the temperatures of 25, 35, 45, and 55 °C starting with the constant initial amounts of $NaBH_4$ (300 mM) and

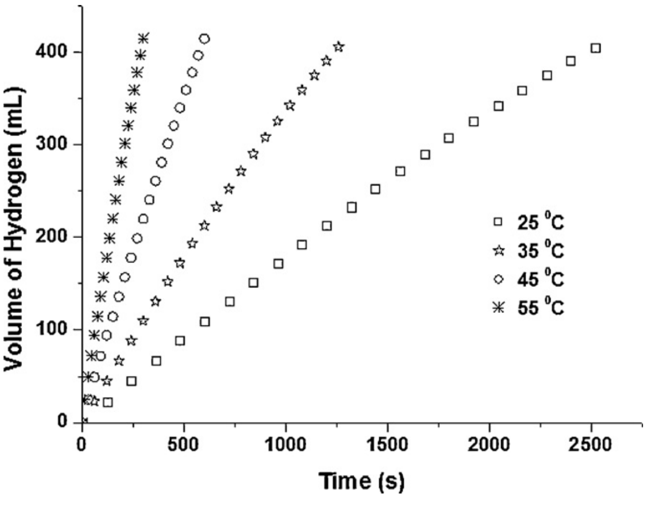

Fig. 5. Plot of the volume of H_2 (mL) versus time (s) for the hydrolysis of $NaBH_4$ (300 mM) catalyzed by Co–Ni–P/Pd-TiO_2 catalyst (25 mg) at the temperatures of 25, 35, 45, and 55 ± 0.5 °C.

Table 1
The values of rate constant k for the hydrolysis of sodium borohydride starting with a solution of 227 mg (300 mM) $NaBH_4$, 25 mg Co–Ni–P/Pd-TiO_2 catalyst, and 10 wt.% NaOH at different temperatures.

Temperature (K)	Rate constant ($mL\,H_2\,s^{-1}$ (mg catalyst)$^{-1}$)
298	0.00692
308	0.01383
318	0.02827
328	0.05653

Co–Ni–P/Pd-TiO_2 catalyst (25 mg) and the maximum H_2 generation rates of ∼460 $mL\,H_2\,min^{-1}$ (g catalyst)$^{-1}$ and ∼3780 $mL\,H_2\,min^{-1}$ (g catalyst)$^{-1}$ were measured at 25 °C and 55 ± 0.5 °C, respectively. Fig. 5 shows the plot of the volume of hydrogen gas generated from the hydrolysis of $NaBH_4$ solution versus time in the presence of Co–Ni–P/Pd-TiO_2 catalyst at various temperatures. The rate constants (Table 1) of hydrogen generation from the hydrolysis of $NaBH_4$ were measured from the linear portions of the plots given in Fig. 5 at four different temperature and used for the calculation of activation energy ($E_a = 57.0\,kJ\,mol^{-1}$) from the Arrhenius plot shown in Fig. 6. This value of activation energy is lower than those reported in the literature for the same reaction using different catalysts like: Ni–Co–B [24], Ru-promoted sulphated zirconia [33], Pt/$LiCoO_2$ [13], Ru/$LiCoO_2$ [27], Ru/C [52], Co–P [30]; but still higher than the activation energy values of some other catalysts like: intrazeolite cobalt(0) nanoclusters [39], Co–B/Ni foam [26], Ni_xB [48], Co/γ-Al_2O_3 [20], Pd-C powder [47], Ru/IR-120 [50], cobalt powder [49], Co–B [22], Co/AC [29], Co–W–B/Ni [28], Ru/IRA-400 [16], and Co–Mn–B nanocomposite [25]. The detailed information on the experimental conditions and catalyst systems used for the hydrolysis of sodium borohydride is given in Table 2.

3.4. Reusability of Co–Ni–P/Pd-TiO_2 catalyst in the hydrolysis of sodium borohydride

The reusability of the catalyst is crucial in the practical hydrogen generation apparatus application. In the present study, the Co–Ni–P catalyst supported on Pd-TiO_2 by electroless deposition method was tested with respect to the reusability in the hydrolysis of $NaBH_4$ in the presence of 10 wt.% NaOH. After the catalytic hydrolysis reaction, the used catalyst was separated from the solution, washed thoroughly with deionized water, dried, and reused in the hydrolysis of $NaBH_4$ (227 mg, 300 mM) solution in the presence of 10 wt.% NaOH. As seen from Fig. 7, the Co–Ni–P catalyst shows good durability in cyclic usage. The catalyst retained up to 86.4% of its initial activity even in the fifth cycle. The slight decrease in catalytic activity in subsequent runs may be attributed to the passivation of the catalyst surface by increasing the concentration of boron products, e.g. metaborate, which decreases the accessibility of active sites [58,59]. Despite this activity loss, it can be concluded that the Co–Ni–P catalyst is isolable, redispersible and yet catalytically active. No further EDX compositional analysis was carried out on the used catalyst.

Table 2
Activation energies and the experimental conditions for different catalyst systems used for the hydrolysis of alkaline sodium borohydride solution.

Catalyst	E_a ($kJ\,mol^{-1}$)	Experimental conditions		Reference
		$NaBH_4$	NaOH	
Fe–Co–B/Ni foam	27	15%	5%	[8]
Pd–C powder	28	0.005 M	pH = 13	[47]
Co–W–B/Ni	29	20%	5%	[28]
Co–B/Ni foam	33	20%	10%	[26]
Co/γ-Al_2O_3	33	5%	5%	[20]
Intrazeolite Co(0) nanoclusters	34	0.15 M	10%	[39]
Co–Ni–B	34	0.025 M	pH = 13	[44]
Ni_xB	38	1.5%	10%	[48]
Co powder	42	0.2 g	10%	[49]
Ru(0) nanoclusters	43	0.15 M	10%	[17]
Co/AC	44	5%	5%	[29]
CoB	45	25%	3%	[22]
Co/C	46	5%	5%	[29]
Ru/IRA-400	47	20%	10%	[16]
Co–Cu–B	50	7%	7%	[46]
Ru/IR-120	50	5%	1%	[50]
BMR07 (Ni based)	52	20%	7%	[51]
Co–Mn–B nanocomposites	55	5%	5%	[25]
Co–B/Attapulgite clay	56	5%	2%	[45]
Ru/IRA-400	56	7.5%	1%	[12]
Co–Ni–P/Pd-TiO_2	57	0.30 M	10%	[This work]
Co–P	60	10%	1%	[30]
Ru/Graphite	61	5%	5%	[42]
Ni–Co–B	62	0.5 g	15%	[24]
Ni210 powder	63	0.2 g	10%	[49]
Ru/C	67	0.993 M	3.75%	[52]
Ru/$LiCoO_2$	68	10%	5%	[27]
Pt/$LiCoO_2$	70	10%	5%	[13]
Ru-promoted sulphated Zr	76	0.661 M	1.3 M	[33]

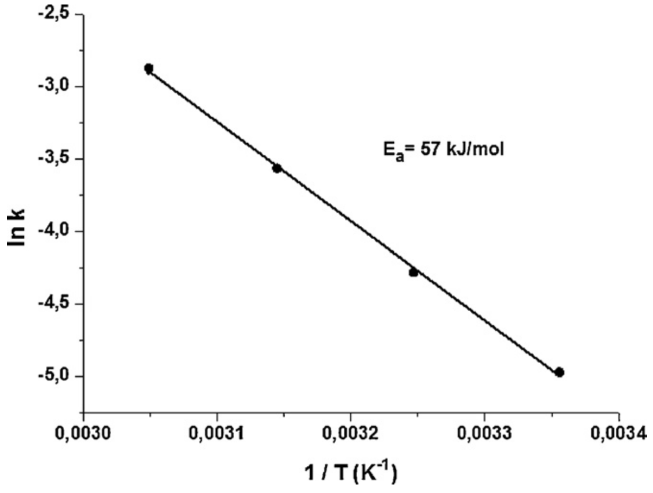

Fig. 6. Arrhenius plot for Co–Ni–P/Pd-TiO_2 (25 mg)-catalyzed hydrolysis of $NaBH_4$ (300 mM) at 25 ± 0.5 °C.

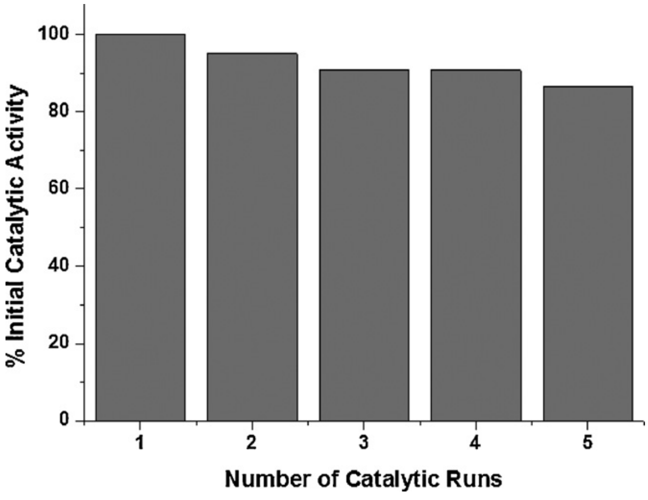

Fig. 7. Reusability tests of the Co–Ni–P/Pd-TiO_2 catalyst in the hydrolysis $NaBH_4$ (300 mM) at 25 ± 0.5 °C.

4. Conclusions

In summary, our study on the kinetics of the hydrolysis of alkaline sodium borohydride catalyzed by Co–Ni–P catalyst supported on Pd-TiO_2 by electroless deposition has led to the following conclusions and insights: The Co–Ni–P/Pd-TiO_2 alloy catalyst prepared by electroless deposition technique was found to be highly active catalyst in the hydrolysis of alkaline $NaBH_4$. Moreover, it is isolable, redispersible, and reusable catalyst. When redispersed in aqueous solution of alkaline $NaBH_4$, it retains 86.4% of its initial catalytic activity even at fifth run. The catalytic hydrolysis of alkaline $NaBH_4$ was found to be first order with respect to catalyst amount and zero order with respect to $NaBH_4$ concentration. This high catalytic activity, low-cost, and reusability of the Co–Ni–P/Pd-TiO_2 catalyst make it a promising candidate to be used as catalyst in developing highly efficient portable hydrogen generation systems using $NaBH_4$ as solid hydrogen storage material.

Acknowledgements

MR thanks to TUBITAK (Research Fellowship-2211) and METU-DPT-OYP program on behalf of Yüzüncü Yıl University. The work was partially supported by National Science Foundation under Engineering Research Center Program no. EEC-0812121.

References

[1] Z. Li, G. Zhu, G. Lu, S. Qiu, X. Yao, J. Am. Chem. Soc. 132 (2010) 1490–1491.
[2] H.B. Dai, L.L. Gao, Y. Liang, X.D. Kang, P. Wang, J. Power Sources 195 (2010) 307–312.
[3] A.J. Hung, S.F. Tsai, Y.Y. Hsu, J.R. Ku, Y.H. Chen, C.C. Yu, Int. J. Hydrogen Energy 33 (2008) 6205–6215.
[4] L. Schlapbach, A. Züttel, Nature 414 (2001) 353–358.
[5] S. Orimo, Y. Nakamori, J.R. Eliseo, A. Züttel, C.M. Jensen, Chem. Rev. 107 (2007) 4111–4132.
[6] V.C.Y. Kong, F.R. Foulkes, D.W. Kirk, J.T. Hinatsu, Int. J. Hydrogen Energy 24 (1999) 665–675.
[7] Q. Xu, M. Chandra, J. Alloys Compd. 446–447 (2007) 729–732.
[8] Y. Liang, P. Wang, H.B. Dai, J. Alloys Compd. 491 (2010) 359–365.
[9] J. Lee, K.Y. Kong, C.R. Jung, E. Cho, S.P. Yoon, J. Han, T.G. Lee, S.W. Nam, Catal. Today 120 (2007) 305–310.
[10] H.I. Schlesinger, H.C. Brown, A.B. Finholt, J.R. Gilbreath, H.R. Hockstra, E.K. Hyde, J. Am. Chem. Soc. 75 (1953) 215–219.
[11] M.M. Kreevoy, R.W. Jacobson, Ventron Alembic 15 (1979) 2–3.
[12] S.C. Amendola, S.L. Sharp-Goldman, M.S. Janjua, N.C. Spencer, M.T. Kelly, P.J. Petillo, M. Binder, Int. J. Hydrogen Energy 25 (2000) 969–975.
[13] Y. Kojima, K. Suzuki, K. Fukumoto, M. Sasaki, T. Yamamoto, Y. Kawai, H. Hayashi, Int. J. Hydrogen Energy 27 (2002) 1029–1034.
[14] C. Wu, H. Zhang, B. Yi, Catal. Today 93–95 (2004) 477–483.
[15] P. Krishnan, T.H. Yang, W.Y. Lee, C.S. Kim, J. Power Sources 143 (2005) 17–23.
[16] Z.T. Xia, S.H. Chan, J. Power Sources 152 (2005) 46–49.
[17] S. Özkar, M. Zahmakıran, J. Alloys Compd. 404–406 (2005) 728–731.
[18] A.M.F.R. Pinto, D.S. Falcao, R.A. Silva, C.M. Rangel, Int. J. Hydrogen Energy 31 (2006) 1341–1347.
[19] K.W. Cho, H.S. Kwon, Catal. Today 120 (2007) 298–304.
[20] W. Ye, H. Zhang, D. Xu, L. Ma, B. Yi, J. Power Sources 164 (2007) 544–548.
[21] Ö. Metin, S. Özkar, Int. J. Hydrogen Energy 32 (2007) 1707–1715.
[22] S.J. Kim, J. Lee, K.Y. Kong, C.R. Jung, I. Min, S.Y. Lee, H.J. Kim, S.W. Nam, T.H. Lim, J. Power Sources 170 (2007) 412–418.
[23] D. Xu, H. Zhang, W. Ye, Catal. Commun. 8 (2007) 1767–1771.
[24] J.C. Ingersoll, N. Mani, J.C. Thenmozhiyal, A. Muthaiah, J. Power Sources 173 (2007) 450–457.
[25] M. Mitov, R. Rashkov, N. Atanassov, A. Zielonka, J. Mater. Sci. 42 (2007) 3367–3372.
[26] H.B. Dai, Y. Liang, P. Wang, H.M. Cheng, J. Power Sources 177 (2008) 17–23.
[27] Z. Liu, B. Guo, S.H. Chan, E.H. Tang, L. Hong, J. Power Sources 176 (2008) 306–311.
[28] H.B. Dai, Y. Liang, P. Wang, X.D. Yao, T. Rufford, M. Lu, H.M. Cheng, Int. J. Hydrogen Energy 33 (2008) 4405–4412.
[29] D. Xu, P. Dai, X. Liu, C. Cao, Q. Guo, J. Power Sources 182 (2008) 616–620.
[30] K.S. Eom, K.W. Cho, H.S. Kwon, J. Power Sources 180 (2008) 484–490.
[31] Ö. Metin, S. Özkar, J. Mol. Catal. A: Chem. 295 (2008) 39–46.
[32] Y. Huang, Y. Wang, R. Zhao, P.K. Shen, Z. Wei, Int. J. Hydrogen Energy 33 (2008) 7110–7115.
[33] U.B. Demirci, F. Garin, J. Mol. Catal. A: Chem. 279 (2008) 57–62.
[34] C.H. Liu, B.H. Chen, C.L. Hsueh, J.R. Ku, M.S. Jeng, F. Tsau, Int. J. Hydrogen Energy 34 (2009) 2153–2163.
[35] O. Akdim, U.B. Demirci, A. Brioude, P. Miele, Int. J. Hydrogen Energy 34 (2009) 5417–5421.
[36] R.P. Alonso, A. Sicurelli, E. Callone, G. Carturan, R. Raj, J. Power Sources 165 (2007) 315–323.
[37] U.B. Demirci, O. Akdim, P. Miele, J. Power Sources 192 (2009) 310–315.
[38] O. Akdim, U.B. Demirci, P. Miele, Acetic Int. J. Hydrogen Energy 34 (2009) 7231–7238.
[39] M. Rakap, S. Özkar, Appl. Catal. B: Environ. 91 (2009) 21–29.
[40] Ö. Metin, S. Özkar, Energy Fuels 23 (2009) 3517–3526.
[41] R. Fernandes, N. Patel, A. Miotello, Appl. Catal. B: Environ. 92 (2009) 68–74.
[42] Y. Liang, H.B. Dai, L.P. Ma, P. Wang, H.M. Cheng, Int. J. Hydrogen Energy 35 (2010) 3023–3028.
[43] H. Tian, Q. Guo, D. Xu, J. Power Sources 195 (2010) 2136–2142.
[44] N. Patel, R. Fernandes, N. Bazzanella, A. Miotello, Thin Solid Films 518 (2010) 4779–4785.
[45] R. Fernandes, N. Patel, A. Miotello, M. Filippi, J. Mol. Catal. A: Chem. 298 (2009) 1–6.
[46] X.L. Ding, X. Yuan, C. Jia, Z.F. Ma, Int. J. Hydrogen Energy 35 (2010) 11077–11084.
[47] N. Patel, B. Patton, C. Zanchetta, R. Fernandes, G. Guella, A. Kale, A. Miotello, Int. J. Hydrogen Energy 33 (2008) 287–292.
[48] D. Hua, Y. Hanxi, A. Xinping, C. Chuansin, Int. J. Hydrogen Energy 28 (2003) 1095–1100.
[49] B.H. Liu, Z.P. Li, S. Suda, J. Alloy Compd. 415 (2006) 288–293.
[50] C.L. Hsueh, C.Y. Chen, J.R. Ku, S.F. Tsai, Y.Y. Hsu, F. Tsau, M.S. Jeng, J. Power Sources 177 (2008) 485–492.
[51] Q. Zhang, Y. Wu, X. Sun, J. Ortega, Ind. Eng. Chem. Res. 46 (2007) 1120–1124.
[52] Z.S. Zhang, W.N. Delgass, T.S. Fisher, J.P. Gore, J. Power Sources 164 (2007) 772–781.
[53] L. Hu, R. Ceccato, R. Raj, J. Power Sources 196 (2011) 69–75.
[54] H.J. Kim, K.J. Shin, H.J. Kim, M.K. Han, H. Kim, Y.G. Shul, K.T. Jung, Int. J. Hydrogen Energy 35 (2010) 12239–12245.
[55] M. Zahmakıran, T. Ayvalı, S. Akbayrak, S. Çalışkan, D. Çelik, S. Özkar, Catal. Today (2010), doi:10.1016/j.cattod.2010.09.022.
[56] D.M.F. Santos, C.A.C. Sequeira, R.F.M. Lobo, Int. J. Hydrogen Energy 35 (2010) 9901–9909.
[57] M. Rakap, E.E. Kalu, S. Özkar, Int. J. Hydrogen Energy 36 (2011) 254–261.
[58] T.J. Clark, G.R. Whittell, I. Manners, Inorg. Chem. 46 (2007) 7522–7527.
[59] C.A. Jaska, T.J. Clark, S.B. Clendenning, D. Groeza, A. Turak, Z.H. Lu, I. Manners, J. Am. Chem. Soc. 127 (2005) 5116–5124.